esa

ECOSPHERE

Modeling the distribution of niche space and risk for a freeze-tolerant ectotherm, *Lithobates sylvaticus*

Megan J. Fitzpatrick,[1,4] Benjamin Zuckerberg,[1,]† Jonathan N. Pauli,[1] Michael R. Kearney,[2] Kimberly L. Thompson,[1] Lawrence C. Werner II,[3] and Warren P. Porter[3]

[1]*Department of Forest and Wildlife Ecology, 1630 Linden Drive, Madison, Wisconsin 53706 USA*
[2]*School of BioSciences, The University of Melbourne, Parkville, Victoria 3010 Australia*
[3]*Department of Integrative Biology, University of Wisconsin-Madison, 250 North Mills Street, Madison, Wisconsin 53706 USA*

Citation: Fitzpatrick, M. J., B. Zuckerberg, J. N. Pauli, M. R. Kearney, K. L. Thompson, L. C. Werner II, and W. P. Porter. 2019. Modeling the distribution of niche space and risk for a freeze-tolerant ectotherm, *Lithobates sylvaticus*. Ecosphere 10(7):e02788. 10.1002/ecs2.2788

Abstract. Many animals depend on stable below-the-snow (subnivium) conditions to survive winter in seasonally cold regions. Freeze-tolerant ectotherms may experience increased ice content and/or energy expenditure in suboptimal subnivium conditions, with implications for overwinter survival and body reserves available for spring reproduction. We used a novel mechanistic modeling approach to explore effects of winter climate on the microclimate conditions, energy expenditure, and ice dynamics of the freeze-tolerant, subnivium-dwelling wood frog (*Lithobates sylvaticus*) in the Upper Midwest and Great Lakes Basin region of the United States. We hypothesized that (1) frogs would experience the greatest energy cost to survive winter in southern regions of our study area, where air temperatures are warmer and shallower snow could allow for increased numbers of freeze–thaw cycles, and (2) frogs would be most vulnerable to lethal freezing in the cold, dry northwest portion of our study region. We found that total winter energy expenditure changed little with latitude because the effect of warmer soil temperatures (higher metabolic rates) to the south was offset by a shorter winter duration. Energy expenditures were greatest in the snowbelts of the Great Lakes, characterized by more persistent snow cover and relatively warm soil temperatures. In contrast, highest ice contents occurred in the northwest of the study region where air temperatures were coldest and snow was shallow. Thus, it appears that wood frogs experience a trade-off between risk of lethal ice content and extensive use of body reserves across geographic space. Simulations showed that interpopulation differences in burrow depth and cryoprotectant concentration can influence risk of lethal ice content and overuse of body reserves prior to spring breeding, and those risks vary in relation to winter climate. Our mechanistic modeling approach is a novel tool for predicting risk and shifting niche space for cold-adapted and subnivium-dependent species.

Key words: energetics; freeze-tolerant; lake effect; mechanistic model; Midwest; niche model; subnivium; wood frogs.

Received 7 February 2019; accepted 8 April 2019; final version received 31 May 2019. Corresponding Editor: Christopher Lepczyk.

[4] Present address: Minnesota Department of Natural Resources, 102 23rd Street NE, Bemidji, Minnesota 56601 USA.

† **E-mail:** bzuckerberg@wisc.edu

Introduction

Winter is a period of energetic deficits and resource limitation, and, therefore, plays a critical role in the survival, distribution, and evolution of organisms in seasonal environments (Campbell et al. 2005, Williams et al. 2015). Many species overwinter in shallow soil, where the insulating

effect of snow provides a relatively warm and stable microclimate—the subnivium—compared to local air temperature (Campbell et al. 2005, Pauli et al. 2013, Williams et al. 2015, O'Connor and Rittenhouse 2016). Among species that overwinter in the subnivium, amphibians appear to be particularly dependent on stable temperatures due to the tight coupling between soil temperatures and metabolic rates and the relatively limited dispersal capacity of many species (Smith and Green 2005). Amphibians, as well as other ectotherms, exposed to freezing conditions must either avoid freezing through supercooling or tolerate freezing through adaptations that regulate ice formation in their tissues (Hillman 2009, Costanzo and Lee 2013). In the wild, freeze-tolerant species may experience energetically expensive freeze–thaw cycles and fluctuating risk of mortality due to deteriorating subnivium conditions and exposure to extreme cold (Sinclair et al. 2013).

Wood frogs (*Lithobates sylvaticus*) are a freeze-tolerant, subnivium-dwelling amphibian ranging from Alaska, USA, to the southern Appalachian Mountains (Dodd 2013). They overwinter in shallow forest soils, beneath leaf litter and debris (Regosin et al. 2003, Baldwin et al. 2006, Dodd 2013, Groff et al. 2016). Like many freeze-tolerant species, wood frogs can survive freezing of up to approximately two-thirds of their body water (Layne Jr. and Lee Jr. 1987, Costanzo and Lee 2013) and rely on colligative cryoprotectants (glucose and urea) to prevent intracellular ice formation and dehydration (Storey and Storey 1984, Costanzo and Lee 2005). Northern populations reach lethal ice content at lower body temperatures than their southern conspecifics due to higher cryoprotectant concentrations (Costanzo et al. 2013, Larson et al. 2014). There is likely a genetic component to these interpopulation differences, as opposed to simply acclimation to different temperatures. Costanzo et al. (2013) found that wood frogs from Alaska and Ohio showed significantly different cryoprotectant responses to the same freezing regime when acclimated to the same conditions for the prior eight weeks. Wood frog survival in colder regions may be further enhanced by burrowing deeper into soil, for example, 3–13 cm below the leaf litter in Alaska (Larson et al. 2014) and Maine (Groff et al. 2016) vs. 3 cm or shallower in Connecticut (O'Connor and Rittenhouse 2016).

Like many freeze-tolerant species, wood frogs do not eat during the winter due to risk of ice nucleation in the gut (Costanzo et al. 2013). Wood frogs also do not eat before breeding, likely due to the absence of insect prey and an inability to digest food in the cold temperatures of early spring (Wells and Bevier 1997, Sinclair et al. 2013). Energy for breeding is consequently dependent on remnants of body reserves acquired in fall (i.e., they are capital breeders; Doughty and Shine 1997), and the survival and reproductive success of wood frogs may be closely tied to climate-influenced winter energy requirements (Reading 2007, Benard 2015). Total energy required to survive the winter increases with winter length and body (soil) temperatures. Wood frogs also incur energy costs (termed threshold costs) with each freeze–thaw cycle, which can have a significant impact on body reserve use (Sinclair et al. 2013). Threshold energy costs are increases in energy expenditure above that predicted by body temperature, and they occur at three points during a freeze–thaw cycle: shortly before the ice formation, at the beginning of ice formation, and immediately following thaw (Sinclair et al. 2013). These increases in metabolic rate are likely related to physiology preparation for and recovery from freezing (Sinclair et al. 2013). In the future, wood frogs may incur additional energy costs due to increased numbers of freeze–thaw cycles and soil warming, or increased risk of reaching lethal ice content due to reduced snow insulation during extreme cold events (Brown and DeGaetano 2011, Sinclair et al. 2013, Williams et al. 2015).

Modeling winter physiology for ectotherms over geographic scales is challenging but critical for quantifying species range limits, predicting range shifts, and identifying populations most sensitive to environmental change. The inclusion of seasonal snowpack in soil temperature calculations is crucial to understanding the physiology of ectotherms wintering in the soil but has not been incorporated into landscape-level models of freeze-tolerant animals. While previous papers have modeled the effects of snow on soil temperatures, soil carbon dynamics, and watershed hydrology (Brown and DeGaetano 2011, Kumar et al. 2013, Lyu and Zhuang 2018), none have modeled spatial variability in snowpack and

subnivium temperatures and tied it to consequences for an animal species.

In this study, we focused on wood frogs in the Upper Midwest and Great Lakes Basin (hereafter UM/GLB) region of the United States under contemporary climate conditions. The UM/GLB study region (Fig. 1) is characterized by low (<0°C) winter air temperatures, particularly in the northwest (Andresen et al. 2014). Snow cover mediates air temperature effects on soil temperatures (Zhang 2005, Thompson et al. 2018), and normal annual snowfall generally increases from south to north, although it declines in the far west (western Minnesota; Andresen et al. 2014). The Great Lakes also have an important effect by creating downwind (south and east) lake effect regions with both milder winter air temperatures and persistent, deep snow cover (Andresen et al. 2014).

Our goal was to identify areas in the study region where overwintering frogs experienced the highest energy requirements and increased likelihood of lethal ice content (>0.67% body water frozen) during winter. We hypothesized that frogs would (1) experience the greatest energy cost in southern regions, where air temperatures are warmer and shallower snow could allow for increased numbers of freeze–thaw cycles, and (2) be most vulnerable to lethal freezing in the northwest portion of our study region

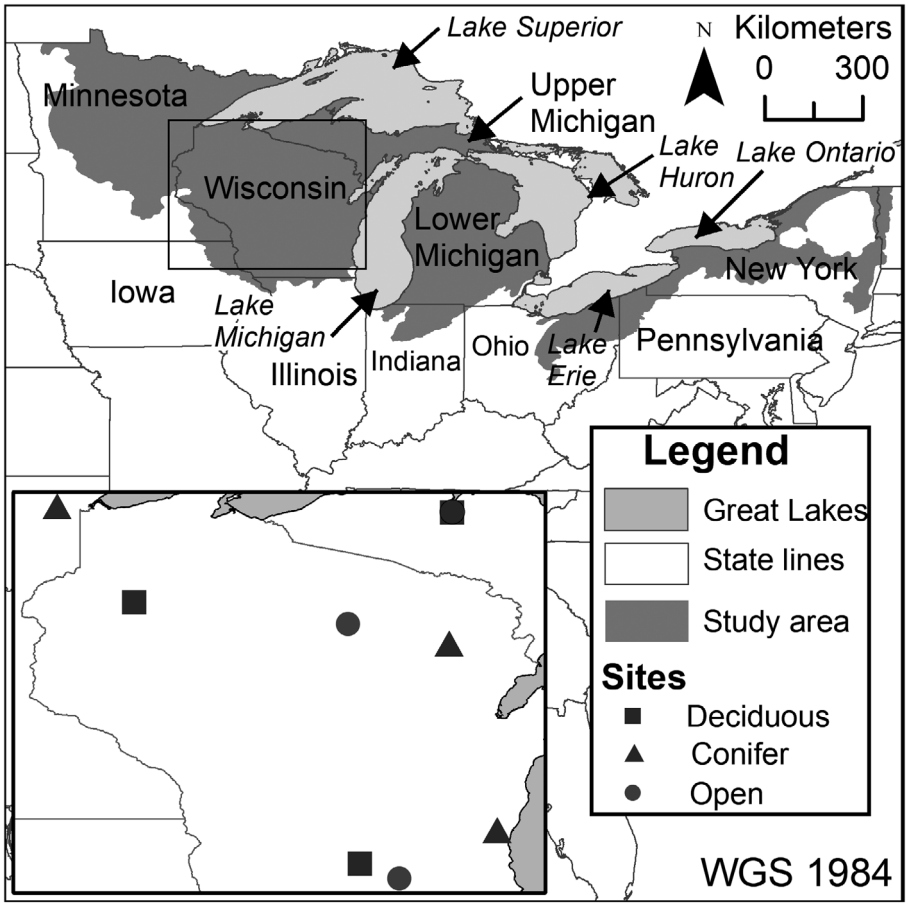

Fig. 1. Study area over which wintering wood frogs were simulated (the Upper Midwest and Great Lakes Landscape Conservation Cooperative) and (inset map) nine field sites in deciduous forest, coniferous forest, or open land cover where weather data were collected to test the microclimate model. An open site and a deciduous site were placed ~500 m apart in Upper Michigan.

characterized by cold air temperatures and low snow cover.

Methods

Model description

Our models are part of the Niche Mapper/NicheMapR (Porter and Mitchell 2006, Kearney and Porter 2017) program suite. The program suite consists of an animal heat-and-mass balance model coupled to a microclimate model, allowing for simulation of animals across geographic space. For this study, we expanded the animal model to simulate transient ice formation and thaw in burrowing ectotherms, along with threshold costs and body reserve (glycogen/lipid) use.

Microclimate model description

We used a modified (Appendix S1) version of the source code for the R (R Core Team 2016) package NicheMapR, version 1.1.3 (Kearney and Porter 2017) to simulate microclimates. The microclimate model is described in detail elsewhere (Kearney and Porter 2017). In short, the model uses physics- and meteorology-based equations to simulate the hourly microclimate conditions that an animal experiences at its local height or soil depth, given daily minimum and maximum air temperature, wind speed, humidity, and cloud cover; daily precipitation; and other landscape metrics (e.g., elevation, slope, land cover). Vertical heat flow through the soil and associated temperatures at 10 soil depths (nodes) are calculated using numerical integration of one-dimensional differential equations for a unit surface area of the soil, given properties of each soil layer. Soil moisture is also computed based on Campbell's (1985) infiltration and redistribution algorithm (Kearney and Maino 2018). The model simulates snow accumulation/melt and snowpack impacts on soil temperatures by treating snow as additional layers of substrate with properties of snow instead of soil.

Microclimate model validation

To validate the microclimate model's simulations of soil temperatures under snowpack, we compared simulated soil surface temperatures for winter 2016–2017 at nine sites across Minnesota, Wisconsin, and Upper Michigan (Fig. 1; Appendix S2) with measured soil temperatures (Thompson et al. 2018; Appendix S2). Sites were in three latitudinal bands (north, middle, and south). Within each band, one site was in deciduous forest, one in coniferous forest, and one in an open area.

We measured daily minimum and maximum air temperatures and wind speeds from three closely spaced (within ~50 m) weather stations from November (prior to first snowfall at each site) to April (after final snowmelt at each site) at each site (Appendix S2). We did not measure snow density but used measured snow depths to choose an input value for modeled snow density (Appendix S2). We obtained daily precipitation and daily minima/maxima of relative humidity and cloud cover from the nearest available weather stations in the NOAA National Climatic Data Center Climate Data Online portal (https://www.ncdc.noaa.gov/cdo-web/, Appendix S2). We also used NOAA station air temperatures and wind speeds to simulate a spin-up period for the soil moisture model and days with missing data due to equipment malfunction (<7% of days at any site; Appendix S2). We adjusted wind speeds for height and forest cover (Appendix S2).

We used generic soil thermal properties from Kearney et al. (2014), including a 5-cm organic cap (O-horizon; Appendix S2). Previous studies have found these values accurately simulate soil temperature profiles at a variety of sites (Kearney et al. 2014). We used literature values of thermal properties to simulate a 5-cm leaf litter layer above the organic cap (Appendix S2). For each site, we used the local soil type's typical soil texture profile from the National Cooperative Soil Survey (Soil Survey Staff 2017) to parameterize the model with depth-specific hydraulic properties for the soil moisture sub-model (Appendix S2). We obtained site elevations (Appendix S2) from Google Earth Pro (version 7.3.1, Google LLC, Palo Alto, California, USA) and simulated all sites as flat (no slope).

Modeled and measured hourly soil temperatures from the snow season (snow depth ≥1 cm) were compared using root mean square deviation (RMSD), normalized root mean square deviation (nRMSD, normalized to the range in measured temperature values), and the coefficient of determination (r^2) and correlation coefficient (r) from a simple linear regression (Kearney et al. 2014, Kearney and Maino 2018). Validation results are shown in Results section below.

Ectotherm model description

The ectotherm model calculates the core temperature of an animal on an hourly basis by solving a heat balance equation between the animal and its environment, given microclimate conditions and information pertaining to the animal's morphology, physiology, and behavior (Beckman et al. 1973, Tracy 1976, Porter and Mitchell 2006). It has previously been used to model aspects of ectotherm physiology that influence amphibian and reptile distribution and movements (Tracy 1976, Kearney et al. 2008, Kearney 2012, Huang et al. 2014, Dudley et al. 2016). For this study, we expanded the ectotherm model to simulate transient ice formation and thaw in burrowing ectotherms, along with threshold costs and body reserve (glycogen/lipid) use. We first describe the modeled timing of frogs' hibernaculum use and then describe how energy expenditure, body reserve use, and ice content are modeled in hibernacula.

Modeled frogs' use of hibernacula.—We simulated wood frogs for a full year (starting in July) and extracted output from the winter season, which we defined as the period when frogs were long-term-restricted to hibernacula. The modeled winter season started during the first hour that the model frog developed ice in its body or during the first hour when snowpack occurred on the ground (whichever came first). The frog remained in the hibernaculum throughout freeze–thaw cycles until the spring season. We defined the spring season as beginning during the first hour when the following criteria were met: (1) The frog was completely thawed, (2) there was no simulated snowpack (i.e., <1 cm snowpack) on the ground, and (3) the simulation was past a user-input threshold date. We used this threshold date to prevent model frog emergence from hibernacula in case of mid-winter snowmelt or warm spells. We chose a threshold date corresponding to the first date for which (1) hibernaculum temperatures were above the frog's crystallization temperature and would remain so for the rest of the simulation, and (2) there would not be any simulated snowpack on the ground for the rest of the season.

Modeled heat balance and ice content in hibernacula.—Frogs were modeled as ellipsoids with volume equal to the combined volume of the limbs and torso. We modeled female and male frogs with average snout-vent lengths of frogs in southwestern Quebec, Canada (Sagor et al. 1998), with relative body dimensions based on measurements of preserved specimens (Appendix S3). We estimated mass (11.6 g female and 8.8 g male) using a mass–length regression (Werner and McCune 1979). Appendix S4: Table S1 shows morphological and physiological parameters used in solving the heat balance equation.

The ectotherm model calculated frog core temperature and ice content on an hourly basis. During each hour, the frog could change either core temperature or ice content (percent of body water frozen). We derived transient equations describing potential for change in temperature and ice content during the hour from a transient heat balance equation incorporating a stored heat term (Appendix S5). Stored heat was directed to changing core temperature or ice formation/melt using two rules. First, ice could form if the frog's core temperature was below its crystallization temperature. For purposes of this study, we defined the crystallization temperature as equal to the frog's equilibrium freezing point, given its body fluid concentration (as defined in Clausen and Costanzo 1990), with an adjustment for bound water content (Appendix S5). That is, we assumed ice nucleation from the surrounding soil would inoculate the frog quickly after it reached its equilibrium freezing point, with essentially no supercooling. Second, we set a limiting value for forming/melting ice based on the frog's core temperature at the beginning of the hour and its osmolality (Clausen and Costanzo 1990: Eq. 2), with an adjustment for bound water (Appendix S5). If more ice would form (or melt) than was possible given the frog's core temperature, stored heat was directed to change frog core temperature rather than ice content.

Core temperature was linked to metabolic rate via a temperature-VCO_2 equation for wood frogs from Sinclair et al. (2013; Appendix S5). VCO_2 was converted to joules given type of body reserves used to fuel metabolism. We usually assumed that frogs used glycogen for non-threshold costs while frozen, fat for non-threshold costs when unfrozen, and glycogen to fuel threshold costs, following Sinclair et al. (2013).

Body mass-normalized threshold energy costs (Sinclair et al. 2013) were stored and summed throughout the winter season with each freeze–

thaw cycle (Appendix S5). Threshold costs occurred when frogs cooled below ~1°C body temperature (the pre-freeze increase), upon ice nucleation, and upon thawing (reaching 0% ice content). Use of body reserves (fat and glycogen) was also stored and summed throughout the winter season (Appendix S5).

Simulations of frogs across the Midwest

For all landscape-level model runs, we simulated a frog for one winter with daily average minimum/maximum air temperatures, wind speeds, cloud over, and humidity conditions from the past decade (2007–2016) at each of ~450,000 locations with ~800 m spacing across the U.S. portion of the Upper Midwest and Great Lakes Landscape Conservation Cooperative (Fig. 1). The conservation region excludes the Adirondack Mountains of New York. In this analysis, we focused on the low-lying areas surrounding the Great Lakes to avoid strong topographic effects and better represent the elevational gradients of our study sites used for microclimate validation. Canada was omitted because daily-scale gridded climate data were unavailable. Because wood frogs overwinter in forested habitat, we restricted simulations to forested sites (sites falling in deciduous, coniferous, shrub/scrub, and woody wetland land cover in the 2011 National Land Cover Database; Homer et al. 2015; Appendix S6). Elevation across the simulated area was obtained from Shuttle Research Topography Mission grids at 90-m resolution and resampled to 30-s resolution (~800 m). Within the range of elevations in our study area, the input elevation value made little difference in model outputs, because site specific weather data inputs accounted for elevation (Appendix S9). Slope and aspect of the ground surface at each point were calculated from elevation data using ArcGIS.

Daily weather data at each of the locations were extracted from spatial grids, including daily minimum and maximum air temperatures from DAYMET (Thornton et al. 2017), humidity from PRISM grids (PRISM Climate Group, http://prism.oregonstate.edu), and wind speeds and cloud cover from NARR (Mesinger et al. 2006; Appendix S6). All raster math and extractions were carried out in R (R Core Team 2016) using the packages raster (Hijmans 2016), rgdal (Bivand et al. 2017), and ncdf4 (Pierce 2017).

We primarily used the same soil thermal properties that we used for single-site microclimate model tests, including a 5-cm layer of leaf litter overlaying a 5-cm organic cap. Simulating the northern deciduous and coniferous sites with varying soil texture properties (clay, loam, silt-loam, and sand) indicated that winter soil temperatures were not very sensitive to the site-specific soil texture-based properties for clay, loam, and silt-loam soil types (Appendix S7). Consequently, we modeled soil texture at all locations as an intermediate texture, loam, rather than acquiring site-specific texture profiles for all locations. Temperatures in sand tended to be ~2–4°C lower than other soil types and responded more quickly to fluctuations in above-snow conditions, such that simulated soil temperatures may overestimate hibernaculum temperatures at sites with high sand content.

We ran several landscape-scale simulations. Each time, we changed one input parameter to bound its potential for variation and assess its impact on wood frog energy expenditure and ice content (Table 1). These parameters were frog size (dimensions and mass), frog hibernaculum depth, frog cryoprotectant concentration/bound water content, type of body reserves used by the frog when not frozen (carbohydrate or lipid), and precipitation conditions. Simulation 1 (Table 1), which included female-sized frog (Appendix S4: Table S1), 5 cm burrow depth, use of lipids as fuel by the frog while not frozen, cryoprotectant levels reflective of midwestern frogs, and precipitation conditions of 2007–2008, was our default setting.

In Simulation 2, we modeled a male-sized frog (Appendix S4: Table S1) to assess effects of smaller body size. We simulated a frog with the female snout-vent length (Appendix S4: Table S1) and a 100% increase in mass (total mass 23.2 g), with a corresponding increase in radial dimensions, to assess the effects of the largest potential body size in Simulation 3.

As our default setting, we assumed frogs used glycogen for non-threshold costs while frozen, fat for non-threshold costs when unfrozen, and glycogen to fuel threshold costs, following Sinclair et al. (2013). In Simulation 4, we assumed glycogen use at all times.

To our knowledge, wood frog hibernaculum depths have not been reported for our study

Table 1. Simulations of frog energetics and ice content across the UM/GLB study region.

Simulation	Frog size†	Frog depth below surface (cm)	Type of body reserves used by frog while frozen	Cryoprotectant levels	Precipitation conditions§
1	Female	5	Lipids	Midwest	2015–2016
2	Male	5	Lipids	Midwest	2015–2016
3	Large female	5	Lipids	Midwest	2015–2016
4	Female	5	Carbohydrates	Midwest	2015–2016
5	Female	10	Lipids	Midwest	2015–2016
6	Female	5	Lipids	Midwest	2007–2008
7‡	Female	5	Lipids	Alaska	2015–2016

† See Appendix S4: Table S1 for sex-specific snout-vent lengths and masses. Large females had twice the mass of the regular female in Appendix S4: Table S1, with a corresponding increase in radial dimensions.

‡ This was not a new simulation but a recalculation of maximum winter ice content based on minimum core temperatures experienced by frogs in Simulation 1.

§ Daily precipitation (mm/d) extracted from DAYMET grids for July 2 of the first year to July 1 of the second year was used as model input. 2007–2008 was the winter with the maximum snow water equivalent (SWE) for the study region, while 2015–2016 was the winter with the minimum SWE.

area. Thus, our default frog hibernaculum depth was below 5 cm of leaf litter based on hibernacula depths reported in Connecticut (maximum of 3 cm below a leaf litter layer <10 cm thick; O'Connor and Rittenhouse 2016), where winter air temperatures are similar to the southern part of our study area. In Simulation 5, we modeled frogs at a 10 cm depth (below 5 cm of leaf litter and 5 cm of soil) based on depths reported in Maine (average 6.8 cm below litter 3.28 cm deep; Groff et al. 2016), where winter air temperatures are similar to the northern region of our study area.

To explore effects of a range of winter precipitation (mm water/d) on the microclimate estimates, we selected winters with the lowest and highest average cumulative snow water equivalent (SWE) across the cells in our study region based on DAYMET grids (Appendix S6). We defaulted to using the minimum SWE year's precipitation values (winter 2015–2016) and used the maximum SWE year's precipitation (winter 2007–2008) in Simulation 6. Precipitation patterns were regional, such that the maximum SWE year's precipitation inputs produced comparatively higher average winter snow depths to the southeast, but lower average winter snow depths in the northwest of our study region (Appendix S4: Fig. S1C, D). We defaulted to using the minimum SWE year's precipitation values to simulate a year with relatively low snowfall. Due to the computationally intensive nature of the simulations (with calculations on an hourly basis), we were unable to simulate wood frogs for the full range of temperatures across the ten years (i.e., 1 January 2007 through 31 December 2016). Consequently, we used daily averages of maximum and minimum temperature values (i.e., average value for each day of year) for the past ten years (2007–2016; Appendix S6) to generate the hourly interpolated values for each simulation day. Daily normals (as opposed to monthly normals) were necessary to simulate day-to-day freeze–thaw cycles for frogs. Soil temperatures are most directly pertinent to wintering frogs and are influenced by a complex combination of factors, including air temperatures and snow depth. Simulating the individual years with the warmest and coldest average winter air temperatures may not result in the warmest and coldest soil temperatures, but we have attempted to bound some climatic variation by running the model with minimum and maximum precipitation conditions to capture variation in snow depth.

To our knowledge, winter body fluid concentrations for frogs in our study area have not been measured. However, plasma glucose concentrations of frozen frogs are available from a comparable latitude (Ottawa, Canada; Storey and Storey 1986). For our default setting, we estimated total plasma osmolality of frozen frogs (Appendix S4: Table S1), following the methods of Costanzo et al. (2013: Table 2) for Ohio frogs, but substituting Ottawa values for glucose (Storey and Storey 1986). To assess effects of cryoprotectant concentration, we recalculated maximum ice contents for frogs with the high

osmolality and bound water contents of Alaskan populations (Costanzo et al. 2013), given simulated minimum frog core temperatures in the Midwest (Simulation 7). We converted model output to rasters (~800 m resolution) and assessed geographic patterns using ArcMap (ArcGIS Desktop 10.5.1; Environmental Systems Research Institute, Redlands, California, USA).

Results

Microclimate model validation

Root mean square deviation at individual sites ranged from 2.15°C to 3.83°C, nRMSD ranged from 8.5% to 15.7%, r^2 ranged from 0.23 to 0.54, and r ranged from 0.48 to 0.74 (Table 2, Fig. 2). Model deviations from measured values tended toward underestimation of soil surface temperature in early to mid-winter (error ≤5°C) and toward predicting stable soil temperatures later into the season due to predicting snowmelt events later in the season than measured snowmelts (Fig. 2; Appendix S2).

Landscape-level simulations

Default conditions (Simulation 1).—The winter season for model frogs in Simulation 1 (Table 1) began between 28 October and 18 December and ended between 11 March and 28 May (Appendix S4: Fig. S3). The start of the modeled winter season was triggered by the first occurrence of snowpack at 59% of sites and by an initial freeze–thaw cycle at 41% of sites (77% of sites where frogs froze).

Table 2. Root mean square deviation (RMSD), normalized root mean square deviation (nRMSD), coefficient of determination (r^2), and correlation coefficient (r) comparing hourly modeled vs. measured soil surface temperatures at nine field sites in the midwestern United States, and average values (Avg.) across sites.

Site	RMSD	nRMSD	r^2	r
N/con	3.28	0.10	0.49	0.60
N/dec	2.96	0.09	0.37	0.70
N/open	3.83	0.10	0.23	0.74
M/con	2.15	0.09	0.33	0.57
M/dec	3.73	0.16	0.54	0.61
M/open	3.41	0.10	0.48	0.60
S/con	3.34	0.11	0.37	0.48
S/dec	2.44	0.11	0.36	0.61
S/open	3.17	0.11	0.37	0.69
Avg.	3.14	0.11	0.39	0.62

Note: Sites were distributed across three latitudinal bands (north, N; middle, M; and south, S) and three cover types (dec, deciduous forest; con, coniferous forest; and open).

Total winter energy expenditure varied widely across the study region, with maximum values ~4 times as large as minimum values (5242–19,630 J/winter; Fig. 3A; see Appendix S4: Fig. S4 for sample hourly metabolic rates and core temperatures). Geographic differences in winter energy expenditure were primarily due to winter length (longer winters equal more energy required) and warmer soil temperatures (warmer soil temperatures produced higher frog body temperatures and consequently higher metabolic rates). We mapped both winter length (Fig. 3C) and daily average metabolic rate (directly related to winter soil temperatures; Fig. 3B) to visualize these separate effects.

Outside of lake effect areas, total winter energy expenditure decreased in southern regions (Fig. 3A) due to a shorter winter season. The decline in total energy expenditure was relatively small, however, because although the winter season shortened, soil temperatures were warmer from north to south (Fig. 3C), soil temperatures warmed from north to south (metabolic rates grew higher; Fig. 3B). Consequently, warmer soil temperatures partially dampened the effects of shorter winter seasons on total winter energy expenditure.

In several lake effect regions, total winter energy expenditure was higher compared to non-lake effect regions of the same latitude (Fig. 3A). The overall highest values of total energy expenditure in our study area occurred on Upper Michigan's Keweenaw Peninsula, in northwestern Lower Michigan, and in the northern lakeshores of Lakes Ontario and Erie (Fig. 3A). High energy expenditure along the southern shore of Lake Superior and in northwestern Lower Michigan (Fig. 3A) was associated with a combination of warmer soil temperatures (higher metabolic rates; Fig. 3B) and long winters (Fig. 3C). Long winters were associated with deeper snow (Appendix S4: Fig. S1C), whereas soil warmth was associated with deep snow and mild air temperatures typical of lakeshore areas (Appendix S4: Fig. S1A–C). For example, in Lower Michigan, warm soil

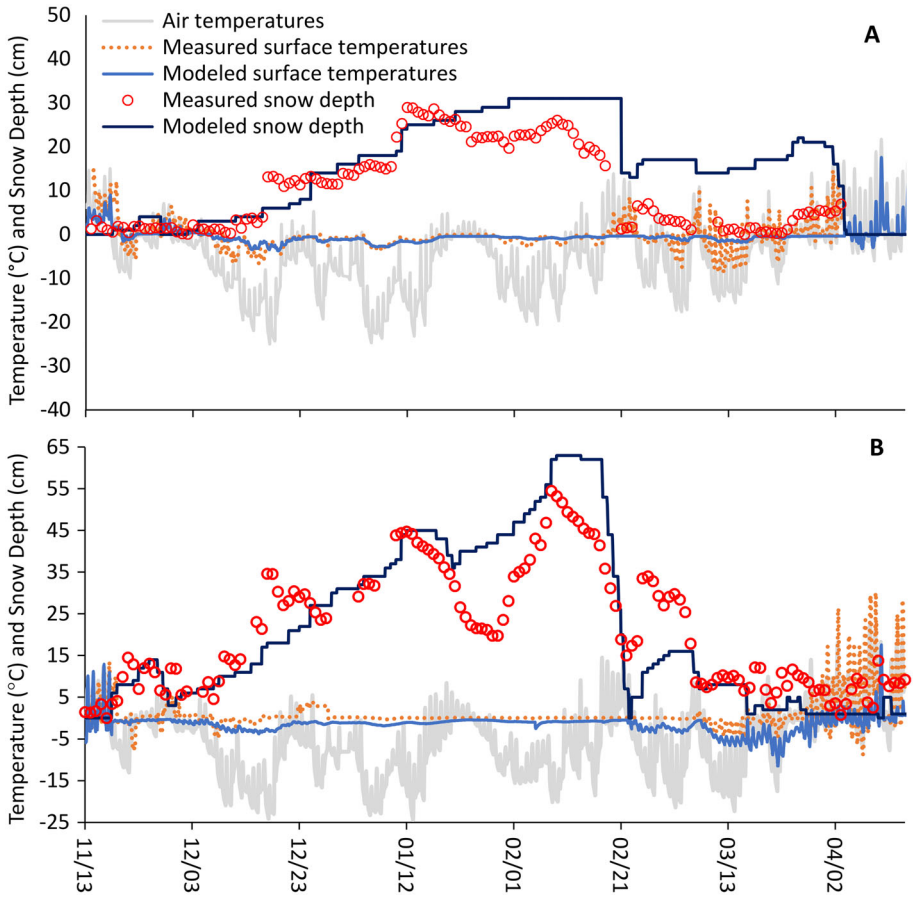

Fig. 2. Measured and model-simulated snow depths and soil surface temperatures for winter 2016–2017 at two of the nine study sites in the midwestern United States. These sites had the lowest (A) and highest (B) root mean square deviation between modeled and measured soil surface temperatures. Site A was in a mid-latitude band with coniferous forest cover. Site B was in the northern latitude band with open forest cover. Appendix S4: Fig. S1 shows results from all nine sites. Air temperatures were measured at 2 m above the ground surface.

temperatures associated with high metabolic rates along the entire coast of Lake Michigan (Fig. 3B), but the highest winter energy expenditures occurred in the north where winter length was also long. In the northern lakeshore regions of Lakes Ontario and Erie, high energy expenditures occurred due to warm soil temperatures (which occurred throughout the southeastern region due to warm air temperatures; Appendix S4: Fig. S1A, B) and long winters in localized regions with deeper snow (Appendix S4: Fig. S1C).

Other notable local patterns included a region of particularly low total energy expenditure in northwestern Minnesota (Fig. 3A) associated with cold soil temperatures and low metabolic rates (Fig. 3B). Cold soil temperatures were associated with shallow snow depths (Appendix S4: Fig. S1C), which are typical of northwestern Minnesota, combined with the broader regional pattern of cold air temperatures at northern latitude (Appendix S4: Fig. S1A, B). Winter energy expenditure increased to the east toward Lake Superior (Fig. 3A) and was associated with increased snow precipitation.

Frogs froze at most sites in northern Minnesota and Wisconsin (Fig. 3D). The highest ice contents occurred in northwestern Minnesota, where shallow snow depths combined with low air and below-the-snow temperatures. Ice content reached lethal levels (>67% body water frozen) in a small number of locations, with a maximum value of 69.4% body water frozen. Frog core temperatures

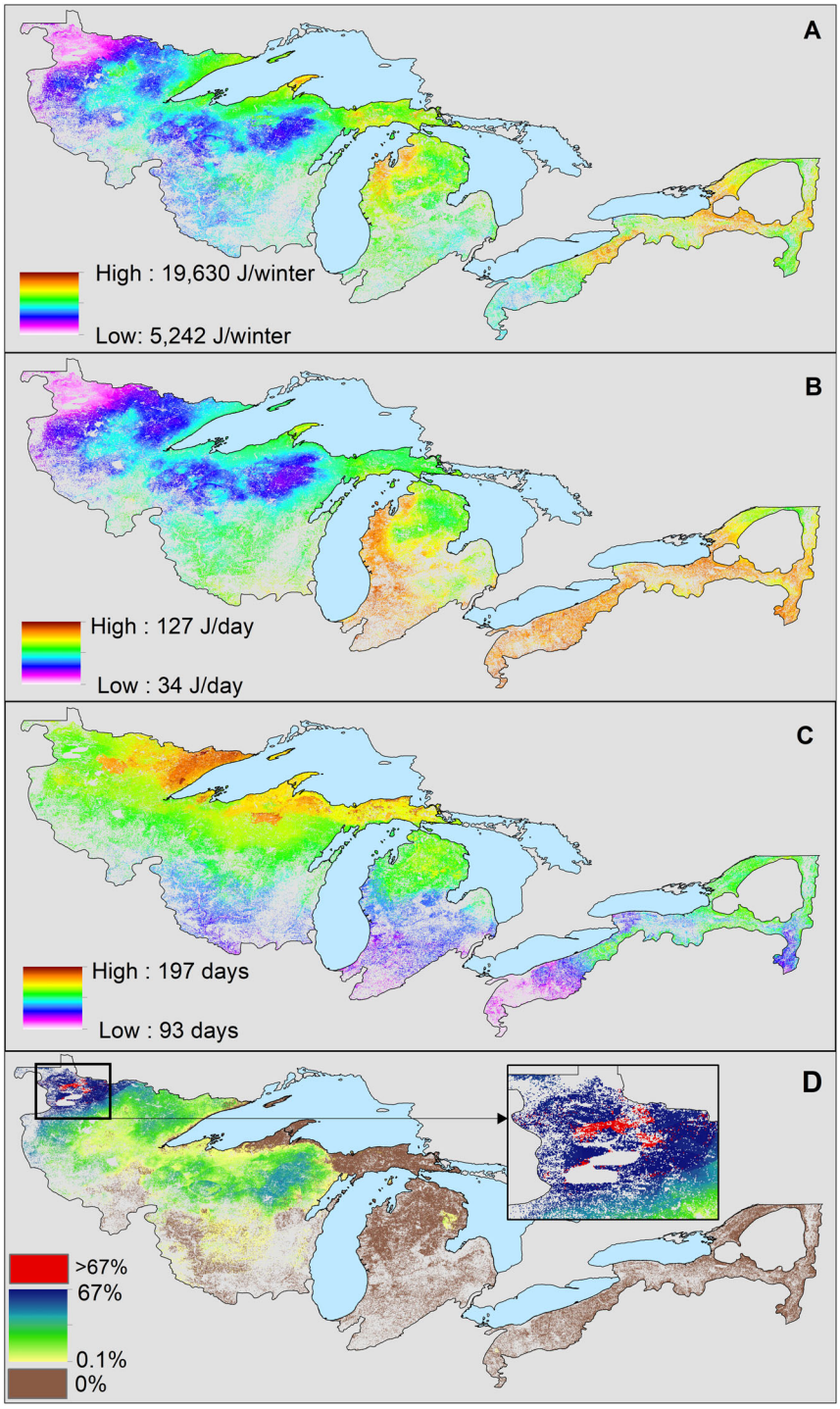

Fig. 3. Modeled (A) total winter energy expenditure (J/winter), (B) daily average winter metabolic rates (J/d), (C) total winter length (d), and (D) maximum ice content (percentage of total body water mass) for a female wood frog in the Upper Midwest and Great Lakes Basin, USA. Inset in panel (D) shows small region where model frogs reached approximate lethal ice content (>67%). Winter refers to the period when frogs are restricted to hibernacula due to ice content in body or existence of snowpack.

did not drop low enough for ice to form throughout most of the southern and eastern areas of our study region under the averaged weather conditions. Warm air temperatures and high snow depths along the southern shore of Lake Superior, along with warming air temperatures to the south and east, formed a boundary around the core area where frogs froze in Minnesota, Wisconsin, and the Upper Michigan. Overall, maximum ice content (Fig. 3D) tended to be higher where winter energy expenditure (Fig. 3A) was lower, with both factors being associated with colder soil temperatures.

Frogs underwent 1–22 freeze–thaw cycles at locations where they froze (Fig. 4C). Threshold costs accounted for a relatively small proportion of total energy expenditure (<5% of total energy expenditure at 98% of sites where frogs underwent freeze–thaw cycles, range 0–13% of energy expenditure; Fig. 4A). At sites where frogs froze, threshold metabolic rates accounted for <1% to 94% of frog carbohydrate consumption (Fig. 4B); however, the distribution of these percentages was right-skewed, with a mean of 22% and a median of 9% carbohydrate consumption going to threshold costs.

Per model assumptions, frogs only used carbohydrate reserves in regions where they froze (Fig. 5A). Carbohydrate use ranged up to 0.34 g. Lipid use showed similar spatial patterns to total energy expenditure, ranging from <0.01 g in regions where frog spent most of the winter frozen to 0.49 g in lake effect regions (Fig. 5B).

Non-default conditions (Simulations 2–6).—Relative geographic patterns in ice content and energy expenditure remained similar throughout all additional simulations. Total winter energy expenditure for male frogs (Simulation 2) was smaller than for females due to smaller body size (Appendix S4: Fig. S5G), but energy expenditure showed similar geographic patterns (Appendix S4: Fig. S5A). Similarly, large females (Simulation 3) had larger total winter energy expenditures, but similar geographic patterns (Appendix S4: Fig. S6A). Male frogs and large female frogs showed similar maximum ice contents to female frogs despite size differences (Appendix S4: Figs. S5J, S6J). Male values differed by <3% body water from female values at 98% of sites where there was a change in values (range of differences −12 to +13.0% of body water). Large females differed by <3% body water from smaller female values at 95% of sites where there was a change in values (range of differences −16.7 to +12.6% of body water).

Total winter energy expenditure showed similar geographic patterns when we assumed carbohydrates instead of lipids fueled unfrozen frogs in Simulation 4 (Appendix S4: Fig. S7A). However, values were smaller and had a smaller range (5218–14,800 J/winter), as expected given the lower energy per unit volume CO_2 for carbohydrates. The reductions in metabolic rate had little impact on frog core temperature and ice content (Appendix S4: Fig. S7I). Carbohydrate requirements ranged from 0.30 to 0.84 g/winter (Appendix S4: Fig. S7E).

When frogs were modeled at 10 cm depth instead of 5 cm (Simulation 5), relative spatial patterns in total energy expenditure remained similar to those at 5 cm depth (Appendix S4: Fig. S8A), but absolute values increased by as much as 4617 J/winter (Appendix S4: Fig. S8G), reflecting the warmer soil temperatures at this greater depth. Due to warmer soil temperatures, the area in which frogs underwent freeze–thaw cycles contracted to include only the area of shallow snow depths in northwestern Minnesota (Appendix S4: Fig. S8D). Maximum ice contents declined by up to 61.4% (Appendix S4: Fig. S8J), reaching a region-wide maximum value of only 58% of body water (Appendix S4: Fig. S8D). Carbohydrate use consequently occurred over a smaller range of sites (Appendix S4: Fig. S8E). Carbohydrate use decreased at many sites despite region-wide increases in metabolic rate (Appendix S4: Fig. S8K) because model frogs spent less time frozen in deeper soil. The maximum value of carbohydrate use (0.27 g/winter) was only 79% of the maximum value at 5 cm depth (0.34 g/winter). However, lipid use increased by up to 0.25 g/winter in accordance with increasing winter energy expenditure (maximum region-wide lipid use 0.56 g/winter; Appendix S4: Fig. S8L). Frogs underwent fewer freeze–thaw cycles at 10 cm depth (up to 8 per winter), with threshold costs accounting for a smaller proportion of total energy expenditure (<4%) and carbohydrate use (range 0–94% of total energy expenditure, but <5% at 92% of sites where frogs froze).

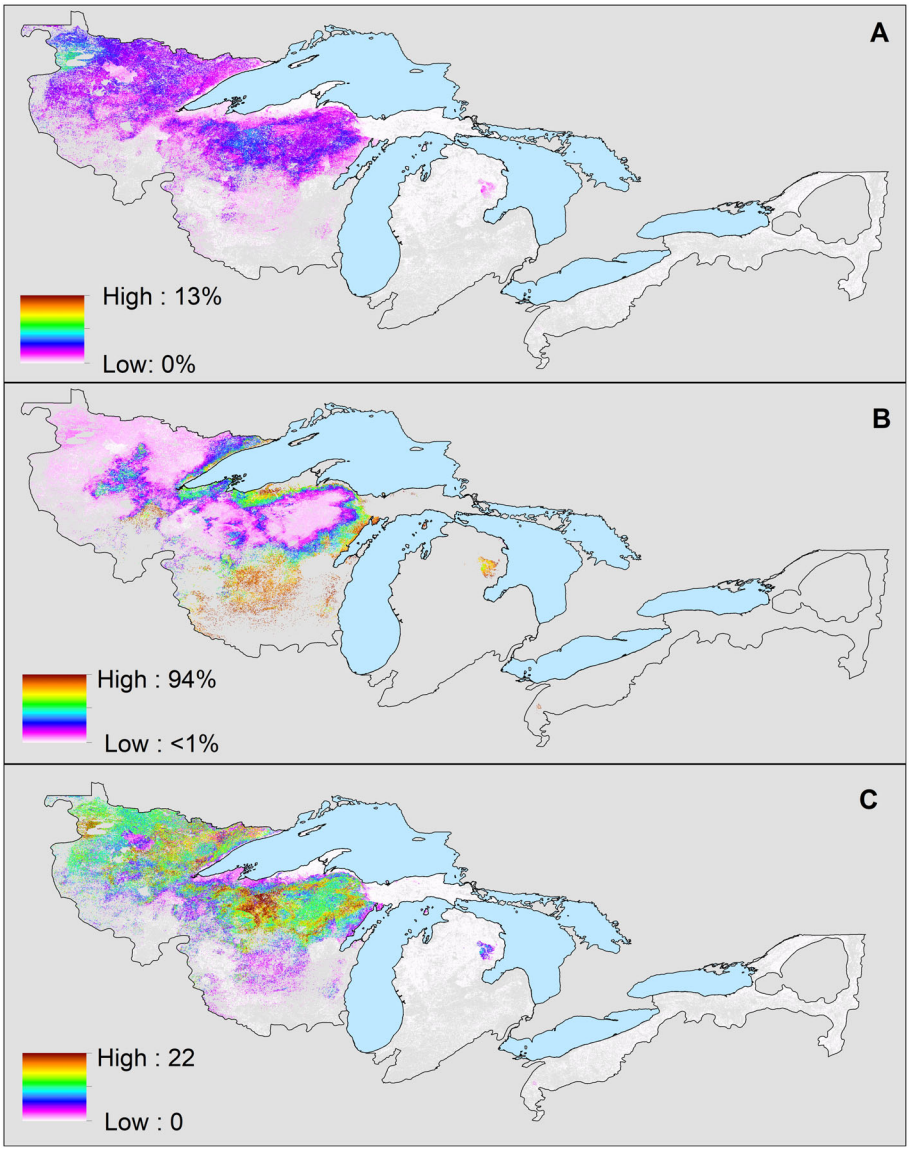

Fig. 4. Modeled (A) threshold costs as percentage of total winter energy expenditure, (B) threshold costs as a percentage of total winter carbohydrate consumption, and (C) number of freeze–thaw cycles for wintering female wood frogs in the Upper Midwest and Great Lakes Basin, USA.

When frogs were modeled under a different year's precipitation conditions (Simulation 6), winter energy expenditures had a larger range (4119–21,780 J/winter), but geographic patterns of energy expenditure remained similar (Appendix S4: Fig. S9A), with highest energy expenditures still in lake effect zones. The increased range in energy expenditure values was associated with decreases in the lowest winter energy expenditures in the northwest, where snow depth declined under this precipitation regime, and increases to the south and east, where snow was deeper under this precipitation regime (Appendix S4: Fig. S9G). Daily average energy expenditures changed in a similar geographic pattern (Appendix S4: Fig. S9H), but change in winter length was more variable through space (Appendix S4: Fig. S9I). With the decrease in snow depth and soil temperatures to the northwest, frogs froze over a wider area and

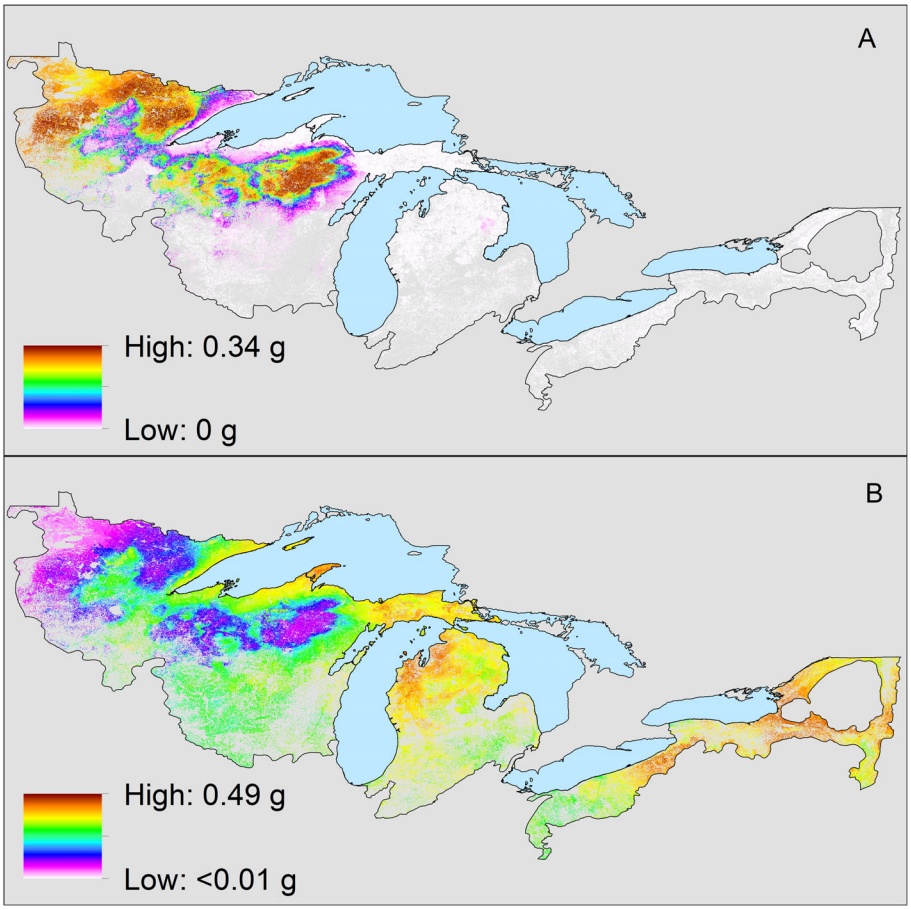

Fig. 5. Modeled mass of (A) carbohydrates(g/winter) and (B) lipids (g/winter) required by wintering female wood frogs in the midwestern United States.

maximum frog ice contents increased (maximum region-wide value 75.6% of body water; Appendix S4: Fig. S9D, J). As a result, geographic patterns in carbohydrate use shifted, with use increasing in some areas due to increased time spent frozen but decreasing in areas where reduction in overall energy expenditure offset the effects of increased freeze time (Appendix S4: Fig. S9K). Lipid use ranged from <0.01 to 0.54 g per winter, generally following patterns of change in total energy expenditure. Frogs underwent similar numbers of freeze–thaw cycles (up to 24). Threshold costs rose to slightly larger proportions of winter energy expenditure (<5% of total winter energy expenditure at 89% of sites where frogs froze, range 0–15% of total winter energy expenditure) and a slightly lower average percentage of total carbohydrate use (mean 8.5% of carbohydrate use at sites where frogs froze, range <1–94% of carbohydrate use).

Maximum ice content that could be reached by frogs with the cryoprotectant levels of Alaskan frogs, given our simulated minimum winter frog core temperatures, is shown in Appendix S4: Fig. S10. The range over which frogs froze was reduced, and maximum ice content decreased from 69.4% to 55.1% (Appendix S4: Fig. S10). These ice contents were calculated at steady state from model output rather than simulated as a transient to reduce computation time and thus may overestimate ice content at some sites.

Discussion

Our simulation results did not support our hypothesis that wood frogs would experience

increased energetic demands in southern regions characterized by warmer temperatures and shallower snow cover. Instead, total winter energy expenditure generally declined with decreasing latitude due to shortening winter season. (The change with latitude was small because higher frog metabolic rates at more southern latitudes partially offset the effects of shorter winters.) Energy expenditure was highest in lake effect snow regions. Increased energy expenditure was a function of both higher metabolic rates associated with warmer soil temperatures and longer winters in lake effect regions. Warmer soil temperatures were associated with deeper snow and warmer air temperatures (especially daily minimum air temperatures) near the lakes.

We found strong support for our hypothesis that wood frogs would be most vulnerable to lethal freezing in the region characterized by cold air temperatures and low snow cover in northwestern Minnesota. Frogs in northwestern Minnesota had the highest simulated ice contents, with maximum ice content reaching just above lethal levels (maximum 69.4%) in a few locations. The northwest was also the region of lowest winter energy requirements, suggesting that wood frogs may experience a trade-off between risk of lethal ice content and extensive use of body reserves in different regions.

Microclimate modeling of the subnivium

The microclimate model predicted winter soil surface temperatures during the snow season with RMSD and nRMSD values similar to previous tests without snow (Kearney et al. 2014). Where the model erred, it tended to underestimate soil temperature by ≤5°C during early to mid-winter and predict overly stable soil temperatures during late winter due to missed snowmelt events. In our geographic simulation, this could lead to overestimation of ice content and underestimation of metabolic rates in early to mid-winter. Prediction of high snow depth and stable soil temperatures for too long into late winter or spring would keep frog temperatures, ice content, and metabolic rate less variable and less dependent on above-snow conditions. Ice content and energy expenditure could be over- or under-predicted, depending on patterns in air temperature. Recent testing and modification of the snow model (M. Kearney, *in preparation*) will improve accuracy of simulated winter soil temperatures in future studies.

In deciduous forests, the model tended to predict a large, rapid melt event near the date that real snowmelt was completed, compensating for missed partial melts when predicting final snow-off date (Appendix S4: Fig. S2). However, in coniferous forests, modeled snow remained on the ground longer than measured snow (Appendix S4: Fig. S2). Modeled snowpack remaining for too long could lead to model frogs remaining in hibernacula for an extended period in coniferous forests. However, the location-specific winter end dates in our landscape-scale simulations (Appendix S4: Fig. S3) matched the Wisconsin Frog and Toad Survey's general observations of Wisconsin wood frog calling phenology of late March to early May in Portage County (mid-latitude Wisconsin), with later dates to the north and earlier dates to the south (Paloski et al. 2014), and breeding date ranges reported in southeastern Michigan (Berven 2009, Benard 2015).

Modeling wood frog physiology at landscape scales

Our finding that threshold costs accounted for a small proportion of total winter energy expenditure was similar to the outcome of a previous modeling study in which threshold costs accounted for <10% of winter energy expenditure at a comparable latitude (Ottawa, Canada; Sinclair et al. 2013). However, in our study, threshold costs tended to account for a smaller proportion of total carbohydrate consumption (mean 22%) than they did for frogs in Ottawa (~60–70%). Threshold costs accounted for smaller proportions of total carbohydrate consumption because frogs in our study were often frozen for a higher proportion of the winter (mean 36% in this study vs. 6–8% in Sinclair et al. 2013) and underwent longer freeze–thaw cycles (up to 150 d long), increasing the amount of carbohydrates consumed in relation to number of freeze–thaw cycles. Longer freezes may have occurred because we used daily air temperatures averaged across years, which may have varied less than the daily temperatures from an individual winter in Sinclair et al. (2013). Sinclair et al. (2013) also based their model on ground surface temperatures measured below 2–5 cm of leaf litter, where

temperatures may have been slightly more variable than the consistent 5 cm depth of our simulations.

Our model predicted that frogs lost 0.22–0.49 g (2–4% body mass) of body reserves (summed fat and glycogen). These values were smaller than measured mass loss in a Connecticut population (average loss 1.42 g; O'Connor and Rittenhouse 2016). Smaller model values are expected because some of the measured mass loss was likely water loss (O'Connor and Rittenhouse 2016), and our results are also comparable to those of an energetics model for wood frogs in Ontario (Sinclair et al. 2013). Body mass-normalized values (Sinclair et al. 2013: Table 3) extrapolate to 0.45–0.49 g lipids/winter and 0.08–0.10 g carbohydrates/winter, or 18–20,000 J/winter, for the body mass assumed in our study (11.6 g female).

Our estimates of body reserve use were high compared to measured values of fat and liver glycogen stores in the literature. Costanzo et al. (2013) measured coelomic fat and liver glycogen stores in winter-acclimated frogs from Ohio and Alaska. If the same percent body fat and glycogen is assumed on a per-mass basis, an 11.6 g frog would contain ~0.01 g fat and 0.10 g glycogen if from Ohio or ~0.002 g fat and 0.34 g glycogen if from Alaska (Appendix S8). In our simulations, maximum carbohydrate use in the UM/GLB was similar to the stores estimated from Alaska frogs, but lipid use was higher than estimated stores at almost all sites, across simulations. Our results suggest that wood frogs may burn a mixture of fats and carbohydrates when unfrozen. Though our simulation assuming carbohydrate use at all times predicted carbohydrate use higher than estimated values from Costanzo et al. (2013) across most of the study region (range 0.30–0.84 g or 3–7% body mass in carbohydrates per winter), wood frogs store additional glycogen in the trunk (Wells and Bevier 1997) and leg (Costanzo et al. 2013) muscles. Future respirometry studies of wood frog freeze–thaw cycles could measure O_2 consumption in addition to CO_2 expiration to explore whether wood frogs rely more heavily on carbohydrates than modeling studies have assumed. We also note that wood frogs may use protein in addition to lipids to meet their energy needs via aerobic metabolism between freezes. Though extensive muscle atrophy may be disadvantageous to spring breeding activities, proteolysis is important in autumn glycogen synthesis and urea acclimation of Alaskan wood frogs (Costanzo et al. 2013, 2015). Future studies could measure size of muscle glycogen and protein stores in relation to whole body mass to assess potential contribution to winter survival.

In the absence of these data, and because coelomic fat and liver glycogen reserves have not yet been measured in wood frogs at our study latitudes, it is difficult to assess where frogs are likely to experience energy limitations to survival or fecundity. However, female wood frog fecundity is negatively associated with winter temperatures in southeastern Michigan, suggesting that warm temperatures may lessen body reserves available for breeding in this area (Benard 2015). In our results, frogs throughout much of our study area (Upper and Lower Michigan, New York, Pennsylvania, northern Ohio) required similar or more body reserves in lake effect regions than in southeastern Michigan. Where frogs require similar or higher levels of body reserves than frogs in Benard (2015), soil temperatures may similarly influence annual variation in reproductive rates and contribute to year-to-year population dynamics. Soil temperature influence may be particularly high in energetically expensive lake effect snow regions.

An important caveat for interpretation of our results is the use of average values for most interannual daily weather conditions (especially air temperature) as model input, which lessened the effects of extreme warm and cold events. In particular, model frogs did not freeze in a large part of our study area. Our results reflect relative patterns in maximum ice content, but actual maximum ice contents are likely to be higher throughout the study region due to the masking of extreme cold events by our use of average weather conditions in the model input. We also note that total winter energy expenditures accounting for greater variability in soil temperature may be higher than those in our study due to Jensen's inequality (Ruel and Ayres 1999). That is, higher variation in body temperature around a given mean temperature over a given period of time results in higher total energy expenditure. We recommend that future studies predicting wood frog energetics and especially ice content include interannual variability in weather

conditions. Future studies might focus on smaller geographic areas, use courser spatial resolution, or make use of high-throughput computing to alleviate computational constraints.

Varying input parameters showed that ice content varied little with frog body size and assumptions about lipid vs. carbohydrate fuel. Ice content did, however, have potential to vary greatly with annual precipitation patterns (which influence snow depth), to decrease with increasing hibernaculum depth, and to decrease with increased cryoprotectant concentration. Variation in these factors may interact to influence frog survival. For example, in precipitation conditions with shallower snow in the northwest, maximum ice contents reached as high as 75.6%. The lethal threshold was nearly crossed even at 10 cm hibernaculum depth under these below-average precipitation conditions, with ice content reaching 66.9% (data not shown). As such, wood frogs in the northwest are likely to reach lethal ice contents in some years, even at burrow depths comparable to those in Alaska (Larson et al. 2014), if they have cryoprotectant concentrations similar to our input values. However, frogs with cryoprotectant concentrations and bound water contents measured in Alaskan frogs remained below lethal ice content. While we do not expect midwestern frogs to have such high bound water and cryoprotectant concentrations, a 10% increase in our assumed input values is enough to keep maximum ice content below two-thirds even at 5 cm depth.

We also note that frog hibernaculum depth may vary across our study region. Intra-population variation in burrow depth affects wood frog mortality (O'Connor and Rittenhouse 2016). Inter- and intra-population variation across our study region could moderate the trade-off between risk of lethal ice content (shallower hibernacula) and higher use of body reserves (deeper hibernacula), with implications for survival (insufficient energy reserves for survival or reduced cryoprotectant concentrations leading to lethal ice contents) and reproductive success (reduced reserves to fuel breeding). For example, simulated frogs in lake effect zones saved 5–15% of total winter energy expenditure at 5 cm depth compared to 10 cm depth, but 5 cm depth may be lethal for frogs in the northwest portion of the study area.

This is the first mechanistic model of both overwintering energy expenditure and transient-state ice content for a freeze-tolerant ectotherm. The inclusion of freeze–thaw dynamics (i.e., percentage of body water frozen) in the ectotherm model represents a significant extension of previous energetics models, incorporating a novel combination of heat balance and phase change equations. By concurrently modeling metabolic rates and ice content, we were able to detect a trade-off between lethal temperatures and high energy requirements across geographic space. The mechanistic nature of the model allowed for an evaluation of potential population-specific behaviors (hibernaculum depths, type of body reserves stored) and physiology (cryoprotectant concentrations and bound water contents) to moderate risks and costs in different regions. Importantly, the mechanistic nature of the microclimate model allows the method to be applied to other regions and time periods. Similarly, the animal model equations (Appendix S5) could be parameterized for other freeze-tolerant ectotherm species in future studies, within the framework of Niche Mapper or other models.

Our results highlight the importance of considering the trade-off between warming soil temperatures and shortening winter season when assessing energy expenditure for subnivium-dependent species at geographic scales. This trade-off may prove critically important over time under future climate change projections. Soil temperatures in the midwestern United States have been projected to increase, while winter length (first to last day with soil frost) is projected to decrease (Sinha and Cherkauer 2010). In the future, temporary or long-term periods of energetic stress may arise if soil temperatures rise too quickly in relation to shortening winters. Further, our analyses indicated the importance of considering annual variability in snow precipitation on lethal ice contents, rather than averaging across years. Annual variability may be particularly relevant as the frequency of extreme weather events increases in the future (Williams et al. 2015). Finally, burrow depth and cryoprotectant concentration strongly influenced the risk of acquiring lethal ice content vs. overusing body reserves. Consequently, there is strong potential for influence of behavioral plasticity (e.g., burrow depth) or physiological traits (e.g., cryoprotectant

concentration) when assessing the vulnerability of cold-adapted species to future climate change.

Acknowledgments

We thank S. Petty and A. Mosloff for their help in data collection for microclimate model validation. We thank the University of Wisconsin-Madison Zoological Museum, especially L. Monahan, for providing wood frog specimens. We thank C. Miller for assistance in measuring museum specimens. Funding for this research was provided by National Science Foundation Macrosystems Biology grant EF-1340632 and by the University of Wisconsin-Madison Department of Forest and Wildlife Ecology. WPP is a co-founder and CEO of Niche Mapper, LLC.

Literature Cited

Andresen, J., S. Hilbert, and K. Kunkel. 2014. Historical climate and climate trends in the midwestern United States. Pages 8–36 *in* J. Winkler, J. Andresen, J. Hatfield, D. Bidwell, and D. Brown, editors. Climate change in the Midwest: a synthesis report for the National Climate Assessment. Island Press, Washington, D.C., USA.

Baldwin, R. F., J. K. C. Aram, and P. G. deMaynadier. 2006. Conservation planning for amphibian species with complex habitat requirements: a case study using movements and habitat selection of the wood frog *Rana sylvatica*. Journal of Herpetology 40:42–453.

Beckman, W. A., J. W. Mitchell, and W. P. Porter. 1973. Thermal model for prediction of a desert iguana's daily and seasonal behavior. Journal of Heat Transfer 95:257–262.

Benard, M. F. 2015. Warmer winters reduce frog fecundity and shift breeding phenology, which consequently alters larval development and metamorphic timing. Global Change Biology 21:1058–1065.

Berven, K. A. 2009. Density dependence in the terrestrial stage of wood frogs: evidence from a 21-year population study. Copeia 2009:328–338.

Bivand, R., T. Keitt, and B. Rowlingson. 2017. rgdal: bindings for the 'Geospatial' Data Abstraction Library. R package version 1.2-15. https://CRAN.R-project.org/package=rgdal

Brown, P. J., and A. T. DeGaetano. 2011. A paradox of cooling winter soil surface temperatures in a warming northeastern United States. Agricultural and Forest Meteorology 151:947–956.

Campbell, G. 1985. Soil physics with basic: transport models for soil-plant systems. Elsevier, Amsterdam, The Netherlands.

Campbell, J. L., M. J. Mitchell, P. M. Groffman, L. M. Christenson, and J. P. Hardy. 2005. Winter in northeastern North America: a critical period for ecological processes. Frontiers in Ecology and the Environment 3:314–322.

Clausen, D. L., and J. P. Costanzo. 1990. A simple model for estimating the ice content of freezing ectotherms. Journal of Thermal Biology 15:223–231.

Costanzo, J. P., M. C. F. do Amaral, A. J. Rosendale, and R. E. Lee. 2013. Hibernation physiology, freezing adaptation and extreme freeze tolerance in a northern population of the wood frog. Journal of Experimental Biology 216:3461–3473.

Costanzo, J. P., and R. E. Lee. 2005. Cryoprotection by urea in a terrestrially hibernating frog. Journal of Experimental Biology 208:4079–4089.

Costanzo, J. P., and R. E. Lee. 2013. Avoidance and tolerance of freezing in ectothermic vertebrates. Journal of Experimental Biology 216:1961–1967.

Costanzo, J. P., A. M. Reynolds, M. C. F. do Amaral, A. J. Rosendale, and R. E. Lee. 2015. Cryoprotectants and extreme freeze tolerance in a subarctic population of the wood frog. PLoS ONE 10:e0117234.

Dodd, K. 2013. *Lithobates sylvaticus*. Pages 637–669 *in* Frogs of the United States and Canada. John Hopkins University Press, Baltimore, Maryland, USA.

Doughty, P., and R. Shine. 1997. Detecting life history trade-offs: Measuring energy stores in 'capital' breeders reveals costs of reproduction. Oecologia 110:508–513.

Dudley, P. N., R. Bonazza, and W. P. Porter. 2016. Climate change impacts on nesting and internesting leatherback sea turtles using 3D animated computational fluid dynamics and finite volume heat transfer. Ecological Modelling 320:231–240.

Groff, L. A., A. J. K. Calhoun, and C. S. Loftin. 2016. Hibernal habitat selection by wood frogs (*Lithobates sylvaticus*) in a northern New England montane landscape. Journal of Herpetology 50:559–569.

Hijmans, R. J. 2016. raster: geographic data analysis and modeling. R package version 2.5-8. https://CRAN.R-project.org/package=raster

Hillman, S. S. 2009. Ecological and environmental physiology of amphibians. Oxford University Press, Oxford, UK.

Homer, C., J. Dewitz, L. Yang, S. Jin, P. Danielson, G. Xian, J. Coulston, N. Herold, J. Wickham, and K. Megown. 2015. Completion of the 2011 National Land Cover Database for the conterminous United States–representing a decade of land cover change information. Photogrammetric Engineering & Remote Sensing 81:345–354.

Huang, S.-P., W. P. Porter, M.-C. Tu, and C.-R. Chiou. 2014. Forest cover reduces thermally suitable habitats and affects responses to a warmer climate

predicted in a high-elevation lizard. Oecologia 175:25–35.

Kearney, M. 2012. Metabolic theory, life history and the distribution of a terrestrial ectotherm. Ecology 26:167–179.

Kearney, M. R., and J. L. Maino. 2018. Can next-generation soil data products improve soil moisture modelling at the continental scale? An assessment using a new microclimate package for the R programming environment. Journal of Hydrology 561:662–673.

Kearney, M., B. L. Phillips, C. R. Tracy, K. A. Christian, G. Betts, and W. P. Porter. 2008. Modelling species distributions without using species distributions: the cane toad in Australia under current and future climates. Ecography 31:423–434.

Kearney, M. R., and W. P. Porter. 2017. NicheMapR – an r package for biophysical modelling: the microclimate model. Ecography 40:664–674.

Kearney, M. R., A. Shamakhy, R. Tingley, D. J. Karoly, A. A. Hoffmann, P. R. Briggs, and W. P. Porter. 2014. Microclimate modelling at macro scales: a test of a general microclimate model integrated with gridded continental-scale soil and weather data. Methods in Ecology and Evolution 5: 273–286.

Kumar, M., D. Marks, J. Dozier, M. Reba, and A. Winstral. 2013. Evaluation of distributed hydrologic impacts of temperature-index and energy-based snow models. Advances in Water Resources 56:77–89.

Larson, D. J., L. Middle, H. Vu, W. Zhang, A. S. Serianni, J. Duman, and B. M. Barnes. 2014. Wood frog adaptations to overwintering in Alaska: new limits to freezing tolerance. Journal of Experimental Biology 217:2193–2200.

Layne Jr., J. R., and R. E. Lee Jr. 1987. Freeze tolerance and the dynamics of ice formation in wood frogs (*Rana sylvatica*) from southern Ohio. Canadian Journal of Zoology 65:2062–2065.

Lyu, Z., and Q. Zhuang. 2018. Quantifying the effects of snowpack on soil thermal and carbon dynamics of the Arctic terrestrial ecosystems. Journal of Geophysical Research: Biogeosciences 123:1197–1212.

Mesinger, F., G. DiMego, E. Kalnay, K. Mitchell, P. C. Shafran, W. Ebisuzaki, D. Jović, J. Woollen, E. Rogers, and E. H. Berbery. 2006. North American regional reanalysis. Bulletin of the American Meteorological Society 87:343–360.

O'Connor, J. H., and T. A. Rittenhouse. 2016. Snow cover and late fall movement influence wood frog survival during an unusually cold winter. Oecologia 181:635–644.

Paloski, R. A., T. L. E. Bergeson, M. Mossman, and R. Hay. 2014. Wisconsin frog and toad survey manual PUB-NH-649. 25 pp. Bureau of Natural Heritage Conservation, Wisconsin Department of Natural Resources, Madison, Wisconsin, USA.

Pauli, J. N., B. Zuckerberg, J. P. Whiteman, and W. P. Porter. 2013. The subnivium: a deteriorating seasonal refugium. Frontiers in Ecology and the Environment 11:260–267.

Pierce, D. 2017. ncdf4: interface to Unidata netCDF. R package version. R package version 1.16. https://CRAN.R-project.org/package=ncdf4

Porter, W. P., and J. W. Mitchell. 2006. Method and system for calculating the spatial-temporal effects of climate and other environmental conditions on animals. Wisconsin Alumni Research Foundation, United States Patent and Trademark Office, USA. https://www.warf.org/technologies/information-technology/software/summary/system-for-calculating-the-spatial-temporal-effects-of-environmental-conditions-on-animals-p01251us.cmsx

PRISM [Parameter-elevation Regressions on Independent Slopes Model] Climate Group, Oregon State University, http://prism.oregonstate.edu

R Development Core Team. 2016. R: a language and environment for statistical computing. R Foundation for Statistical Computing, Vienna, Austria.

Reading, C. J. 2007. Linking global warming to amphibian declines through its effects on female body condition and survivorship. Oecologia 151: 125–131.

Regosin, J. V., B. S. Windmiller, and J. M. Reed. 2003. Terrestrial habitat use and winter densities of the wood frog (*Rana sylvatica*). Journal of Herpetology 37:390–394.

Ruel, J. J., and M. P. Ayres. 1999. Jensen's inequality predicts effects of environmental variation. Trends in Ecology & Evolution 14:361–366.

Sagor, E. S., M. Ouellet, E. Barten, and D. M. Green. 1998. Skeletochronology and geographic variation in age structure in the wood frog, *Rana sylvatica*. Journal of Herpetology 32:469–474.

Sinclair, B. J., J. R. Stinziano, C. M. Williams, H. A. MacMillan, K. E. Marshall, and K. B. Storey. 2013. Real-time measurement of metabolic rate during freezing and thawing of the wood frog, *Rana sylvatica*: implications for overwinter energy use. Journal of Experimental Biology 216:292–302.

Sinha, S., and K. A. Cherkauer. 2010. Impacts of future climate change on soil frost in the midwestern United States. Journal of Geophysical Research 115:229–252.

Smith, M., and D. Green. 2005. Dispersal and the metapopulation paradigm in amphibian ecology and conservation: Are all amphibian populations metapopulations? Ecography 28:110–128.

Soil Survey Staff. 2017. Natural Resources Conservation Service, United States Department of

Agriculture. Web Soil Survey. https://websoilsurvey.sc.egov.usda.gov/

Storey, K. B., and J. M. Storey. 1984. Biochemical adaption for freezing tolerance in the wood frog, rana sylvatica. Journal of Comparative Physiology B 155:29–36.

Storey, K. B., and J. M. Storey. 1986. Freeze tolerant frogs: cryoprotectants and tissue metabolism during freeze–thaw cycles. Canadian Journal of Zoology 64:49–56.

Thompson, K., B. Zuckerberg, W. Porter, and J. Pauli. 2018. The phenology of the subnivium. Environmental Research Letters 13:064037.

Thornton, P. E., M. M. Thornton, B. W. Mayer, Y. Wei, R. Devarakonda, R. S. Vose, and R. B. Cook. 2017. Daymet: daily surface weather data on a 1-km grid for North America, version 3. ORNL DAAC, Oak Ridge, Tennessee, USA. https://doi.org/10.3334/ORNLDAAC/1328

Tracy, C. R. 1976. A model of the dynamic exchanges of water and energy between a terrestrial amphibian and its environment. Ecological Monographs 46:293–326.

Wells, K. D., and C. R. Bevier. 1997. Contrasting patterns of energy substrate use in two species of frogs that breed in cold weather. Herpetologica 53:70–80.

Werner, J. K., and M. B. McCune. 1979. Seasonal changes in anuran populations in a northern Michigan pond. Journal of Herpetology 13:101–104.

Williams, C. M., H. A. L. Henry, and B. J. Sinclair. 2015. Cold truths: how winter drives responses of terrestrial organisms to climate change. Biological Reviews 90:214–235.

Zhang, T. 2005. Influence of the seasonal snow cover on the ground thermal regime: an overview. Reviews of Geophysics 43:1–23.

Supporting Information

Additional Supporting Information may be found online at: http://onlinelibrary.wiley.com/doi/10.1002/ecs2.2788/full